Coherent imaging of nanoscale plasmon patterns with a carbon nanotube optical probe

R. Hillenbrand[a)]
Nano-Photonics Group, Max-Planck-Institut für Biochemie, 82152 Martinsried, Germany

F. Keilmann
Abteilung Molekulare Strukturbiologie, Max-Planck-Institut für Biochemie, 82152 Martinsried, Germany

P. Hanarp and D. S. Sutherland
Department of Applied Physics, Chalmers University of Technology, 41296 Göteborg, Sweden

J. Aizpurua
National Institute of Standards and Technology, Gaithersburg, Maryland 20899-8423

(Received 4 April 2003; accepted 13 May 2003)

We introduce a carbon nanotube as optical near-field probe and apply it to visualize the plasmon fields of metal nanostructures in both amplitude and phase at 30 nm resolution. With 91 nm Au disks designed for fundamental plasmon resonance, we observe the antiphase optical fields near two pole regions that are evidence of dipolar oscillation, in good agreement with theoretical field patterns. This opens the door to phase-sensitively map optical propagation and storage in photonic crystals and nanooptic resonators or circuits, in particular to verify coherent control of plasmon polaritons. © *2003 American Institute of Physics.* [DOI: 10.1063/1.1592629]

An intriguing approach to overcome the optical diffraction limit explores the plasmon-polariton excitation in metal nanostructures[1–3] where light excites collective electron oscillations inducing strong scattering and enhanced, locally confined optical near fields. The enhanced intensity causes colossal surface-enhanced Raman scattering (SERS)[4] and enables fascinating nonlinear devices.[5] Plasmon resonance has already allowed photonic applications of guiding[2] and controlling[1,6] light on a subwavelength scale. The optical phase is essential in coherent control applications, e.g., for controlling the spatial distribution of the plasmon energy within nanostructures.[7] Phase-contrast near-field optical imaging has already allowed tracking waveguide modes[8] and viewing particle plasmons[9] yet with the limited resolution of aperture probes. To understand nanoscale optical phase effects and to enable ultrahigh resolution imaging of plasmon fields we introduce and demonstrate carbon nanotube tips (CNTs)[10,11] to function as low-perturbation optical probes in our phase-sensitive, scattering-type near-field optical microscope (*s*-SNOM).

In *s*-SNOM a focused light beam illuminates a sharp probe,[12–15] usually the metallized tip of an atomic force microscope (AFM) that is scanned in close proximity to a sample surface. Light scattered from the tip measures the near-field interaction between tip and sample, and thus maps the local refractive index,[14,16] the absorption,[13] or field patterns,[17] simultaneously with topography. The optical resolution of *s*-SNOMs is roughly equal to the curvature radius a of the tip apex and has reached below 10 nm.[15,18] Common metal tips can be expected (since they have very large conductivity even at optical frequencies) to perturb plasmon fields because they can induce resonance shift, multipole excitation, and damping.[3] As possibly less perturbing alternative we introduce here a CNT optical near-field probe.

We use a 4 μm long CNT bundle (Fig. 1) mounted on the Si tip of a conventional AFM cantilever (supplied by npoint, Madison, WI). The CNT is found to permit stable tapping-mode (frequency $\Omega=330$ kHz) mechanical operation and topographic imaging. For optical imaging we focus illuminating light at $\lambda=633$ nm wavelength onto the CNT, with incident wave vector k_i at 30° from the y direction, and with the field E_i polarized in the $y-z$ plane (Fig. 1). Backscattered light is collected with the same lens and analyzed interferometrically. Heterodyne detection is used for the simultaneous imaging of both the amplitude $|E|$ and the phase φ of the scattered near field $E \propto \alpha_{\text{eff}} E_i$.[16] An analytic expression for α_{eff} can be derived from treating the scattering, in dipolar

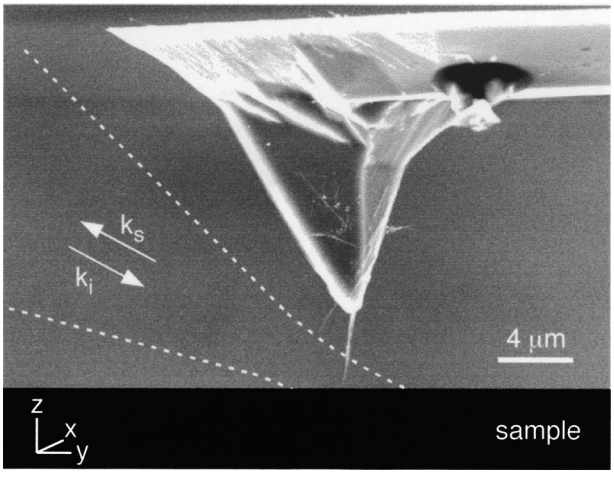

FIG. 1. Scanning electron microscopy image of the CNT probe ontop an AFM tip, taken after use in the described optical near-field experiments. Superimposed is the shape of the illuminating HeNe laser beam (to scale), and the backscattered beam which maps the optical near-field image, simultaneously with the topographical imaging of the scanned sample.

a)Electronic mail: hillenbr@biochem.mpg.de

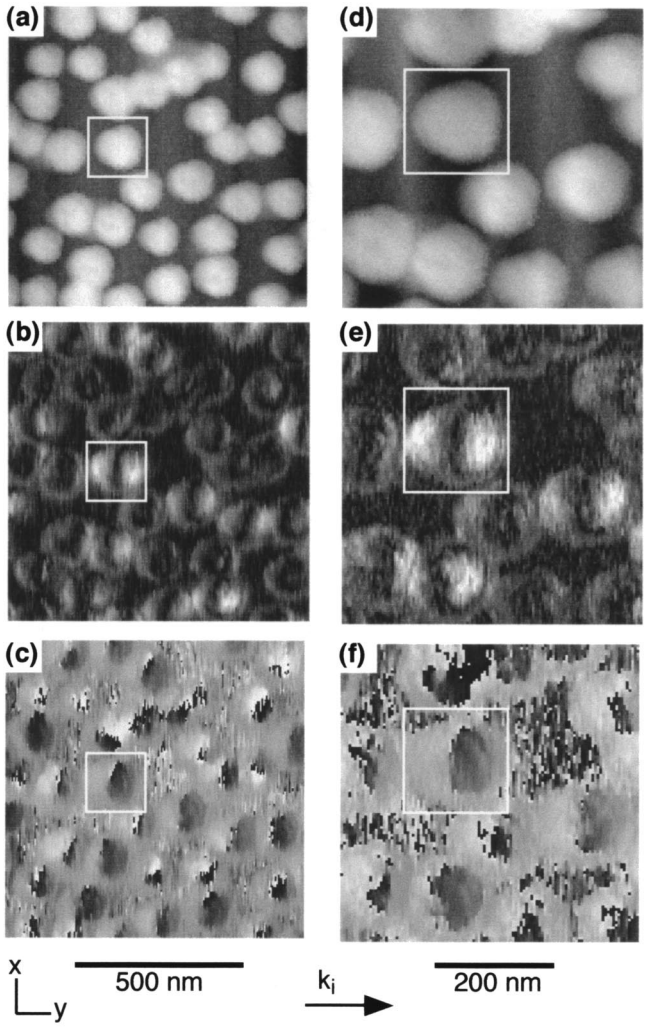

FIG. 2. Images of Au islands on glass taken with the CNT probe. (a) Topography (25 nm full scale) with (b) simultaneously recorded optical amplitude E_2 and (c) optical phase φ_2 (360° full scale); (d)–(f) repeat with reduced scan area showing (d) topography with (e) simultaneously recorded optical amplitude E_3 and (f) optical phase φ_3. k_i marks the direction of the incident light.

approximation, as the near-field interaction between a tip dipole and a mirror dipole induced in the sample.[16] A nonlinear distance dependence of the near-field scattering, expressed in α_{eff}, occurs also with CNTs and is utilized to suppress the unavoidable strong background scattering. As discussed earlier,[16] the tapping motion at frequency Ω modulates the distance z and induces harmonics in the near-field scattering signal but not in the background signal, and therefore, demodulating the optical detector signal at a harmonic frequency $n\Omega$ with $n \geqslant 2$ allows us to extract a background-free near-field signal amplitude $|E_n|$ and phase φ_n.

To verify CNT optical near-field imaging, and also to characterize the coherent, phase-and-amplitude response of a basic building block of a nanophotonic system[1] we fabricate circular nanodisks and validate our experimental results by comparison with a quantitative numerical prediction. The resonance wavelength of the disks is designed to be 633 nm through choice of their size and aspect ratio. Samples with disk-shaped Au islands (91 nm diam., 20 nm height) on glass are made by colloidal lithographic masking[19] and plasma etching. Far-field optical extinction spectra exhibit a slightly

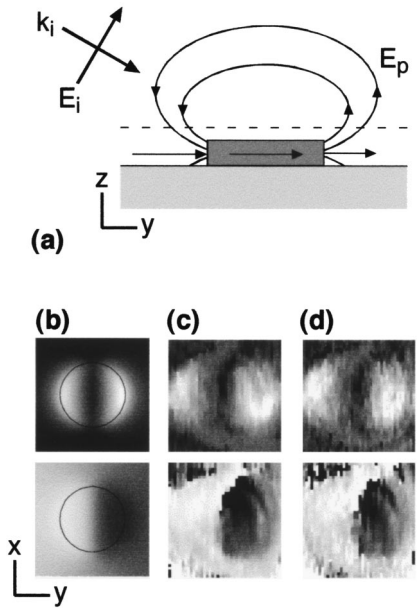

FIG. 3. Evidence of dipolar plasmon oscillation resonantly induced by 633 nm light in a 91 nm diam. 20 nm high Au disk on glass. (a) Schematic side view of incident plane wave and particle fields. (b)–(d) Top view of field distribution (160 nm×160 nm) in amplitude (upper row) and phase (lower row, 180° full scale): (b) exact theory result for the z component of the total field 10 nm above the disk as marked by the dashed line in (a); (c) experimental s-SNOM images E_2 and φ_2 using CNT; (d) experimental s-SNOM images E_3 and φ_3 using CNT, taken from Figs. 2(e) and 2(f).

shifted resonance at 624 nm wavelength with 88 nm full width at half maximum (ensemble averaged).

Evidently near-field imaging with the CNT yields stable, repeatable nanoscopic optical contrasts (Fig. 2). In topography [Figs. 2(a) and 2(d)] the disks appear quite regular in size and shape, 20 nm high and about 140 nm in diameter, a broadening due to the tip radius a≈25 nm. Near-field images taken at demodulation order $n=2$, 3 [Figs. 2(b), 2(c), 2(e), and 2(f)] reveal a characteristic optical pattern for the brighter nanodisks, in amplitude as well as in phase, that is different from topography and shows subparticle-size detail. Here the optical amplitude systematically exhibits two bright areas, separated by a dark zone, which are aligned in y direction, i.e., along the projection of the incident beam k_i (Fig. 1). The phase images show, interestingly, that both areas oscillate essentially out of phase [Figs. 2(c) and 2(f)]. The many other disks which appear much darker, close to noise [Figs. 2(b) and 2(e)], testify to the strong dependence of the plasmon resonance on small differences in size, shape, or environment long known from ensemble-averaged measurements.[3] Obviously the individual resonances are shifted above or below 633 nm wavelength. Figures 2(e) and 2(f) indeed reproduce the characteristic optical pattern at higher magnification (i.e., using a reduced scan range), in amplitude as well as in phase contrast, which demonstrates the high quality of CNT optical imaging. The resolution is of the order of the CNT bundle diameter and should be improvable to about 1 nm by employing single-walled CNTs. This could enable to correlate in a single measurement the optical response with the detailed size and shape of individual particles, even at very close spacing.

The optical pattern is evidence of a highly symmetric optical plasmon oscillation mode of a disk that measures

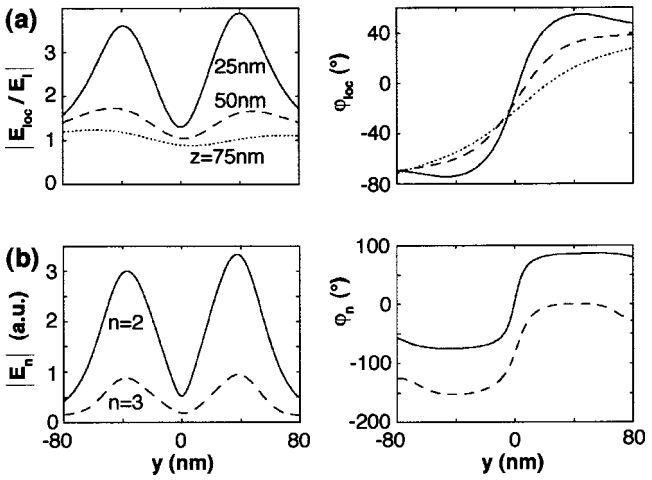

FIG. 4. Calculated field E_{loc} (a) and result of $n=2$ and $n=3$ harmonic signal demodulation (b), for a 91 nm diam., 20 nm high Au disk on glass centered at $x=0$, $y=0$, $z=-10$ nm. (a) Amplitude $|E_{\mathrm{loc}}/E_i|$ and phase φ_{loc} of the local fields z component at different heights at $x=0$. (b) s-SNOM signal amplitude $|E_n|$ and phase $|\varphi_n|$ for sinusoidal tip oscillation between $z=25$ and 75 nm, tip diameter $a=25$ nm, and demodulation order $n=2$ and $n=3$.

only $\lambda/7$ in diameter [Fig. 3(a)]. To understand its origin, the incident light E_i can be thought to preliminary induce a particle dipole oriented parallel to the projection of k_i in the disk plane, whose field E_p adds to the incident field E_i. Thus the field E scattered by the tip becomes $E \propto \alpha_{\mathrm{eff}} E_{\mathrm{loc}}$ where $E_{\mathrm{loc}} = E_i + E_p$ is the local optical field at the tip apex. Because only z components are imaged[17,20] we expect bright polar regions oscillating essentially out of phase. To predict the local field E_{loc} we perform an exact electrodynamic calculation. Using the boundary charge method the electric field is expressed in terms of charges and currents distributed on the surface of the disk, which are determined self-consistently in the presence of the external incident light field by discretizing the linear integral equations arising from the customary boundary conditions.[21] The result [Fig. 3(b)] indeed yields a dipolar pattern with symmetry axis along k_i and bright regions near the poles that show a phase difference of 145° (note 180° is to be expected only for fields $E_p \gg E_i$). Comparing the theoretical near-field pattern [Fig. 3(b)] with experimental data [Figs. 3(c) and 3(d)] we find great similarity although the latter are obtained by harmonic signal demodulation at $n=2$, 3. That our experimental procedure can indeed qualitatively determine the particles near-field pattern is backed by the following analysis. Figure 4(a) displays the calculated local field and its phase in different heights above the sample while Fig. 4(b) shows the theoretical response of our s-SNOM. For the latter we calculate the time course of the scattered field $E=E[z(t)]$ taking into account a sinusoidal tip oscillation between $z=25$ and 75 nm. Subsequent Fourier analysis yields the optical signal $E_n=|E_n|e^{i\varphi_n}$. Comparing local field E_{loc} and s-SNOM signal E_n confirms that the optical pattern qualitatively persists independently of the harmonic demodulation order. Thus, the good agreement between theoretical simulation—which does not include a possible influence of the tip on E_p—and the experimental near-field patterns lets us further conclude that near-field probing by a CNT does not perturb the optical oscillation mode of the disk significantly.

Altogether our results are evidence that a CNT probe allows to image both optical amplitude and phase at nanoscale resolution. Our results with plasmon-resonant gold disks certify that the CNT tool will reliably analyze the nanoscale field patterns of future nanooptical circuits. Gernerally any CNT probing can be enhanced by the power of light spectroscopies, such as fluorescence,[22] infrared,[13,14] and Raman[23] for material-specific analysis on the nanometer scale. A principal advantage of CNTs for near-field microscopy is the elongated shape that will also facilitate probing of the plasmon fields of nanoscale pinholes with enhanced transmission[24] and of deep gratings, or the extremely strong optical fields that exist in deep, hard-to-access gaps between plasmon-resonant particles. While our former experiment with a Si tip could not reach into the maximum field region,[17] we expect that single-wall CNTs would be well suited. We further suggest (bio)chemically functionalized CNTs[25] for optical sensing to obtain mechanical, optical, and chemical information simultaneously.

The authors thank F. J. García de Abajo for providing calculation software, and T. Taubner and R. Saykally for stimulating discussions. Supported by DFG and BMBF. Use of the equipment does not constitute an endorsement by NIST.

[1] J. R. Krenn, A. Dereux, J. C. Weeber *et al.*, Phys. Rev. Lett. **82**, 2590 (1999).
[2] M. Salerno, J. R. Krenn, B. Lamprecht *et al.*, Opto-Electron. Rev. **10**, 217 (2002).
[3] U. Kreibig and M. Vollmer, *Optical Properties of Metal Clusters* (Springer, Berlin, 1995).
[4] H. Xu, E. J. Bjerneld, M. Käll *et al.*, Phys. Rev. Lett. **83**, 4357 (1999).
[5] I. I. Smolyaninov, C. C. Davis, and A. V. Zayats, Appl. Phys. Lett. **81**, 3314 (2002).
[6] J. Müller, C. Sönnichsen, H. V. Poschinger *et al.*, Appl. Phys. Lett. **81**, 171 (2002).
[7] M. I. Stockmann, S. V. Faleev, and D. J. Bergmann, Phys. Rev. Lett. **88**, 67402 (2002).
[8] M. L. M. Balistreri, H. Gersen, J. P. Korterik *et al.*, Science **294**, 1080 (2001).
[9] J. Prikulis, H. Xu, L. Gunnarsson *et al.*, J. Appl. Phys. **92**, 6211 (2002).
[10] H. Dai, J. H. Hafner, A. G. Rinzler *et al.*, Nature (London) **384**, 147 (1996).
[11] T. Larsen, K. Moloni, F. Flack *et al.*, Appl. Phys. Lett. **80**, 1996 (2002).
[12] A. Lahrech, R. Bachelot, P. Gleyzes *et al.*, Opt. Lett. **21**, 1315 (1996); Y. Inouye and S. Kawata, *ibid.* **19**, 159 (1994).
[13] B. Knoll and F. Keilmann, Nature (London) **399**, 134 (1999).
[14] R. Hillenbrand, T. Taubner, and F. Keilmann, Nature (London) **418**, 159 (2002).
[15] F. Zenhausern, Y. Martin, and H. K. Wickramasinghe, Science **269**, 1083 (1995).
[16] R. Hillenbrand and F. Keilmann, Phys. Rev. Lett. **85**, 3029 (2000).
[17] R. Hillenbrand and F. Keilmann, Appl. Phys. B: Lasers Opt. **73**, 239 (2001).
[18] R. Hillenbrand and F. Keilmann, Appl. Phys. Lett. **80**, 25 (2002).
[19] P. Hanarp, D. S. Sutherland, J. Gold *et al.*, Colloids Surf., A **214**, 23–36 (2003).
[20] B. Knoll and F. Keilmann, J. Microsc. **194**, 512 (1999).
[21] F. J. García de Abajo and A. Howie, Phys. Rev. B **65**, 115418 (2002).
[22] J. T. Yang, G. A. Lessard, and S. R. Quake, Appl. Phys. Lett. **76**, 378 (2000).
[23] R. M. Stöckle, Y. D. Suh, V. Deckert *et al.*, Chem. Phys. Lett. **318**, 131 (2000).
[24] T. W. Ebbesen, H. J. Lezec, H. F. Ghaemi *et al.*, Nature (London) **391**, 667 (1998).
[25] S. S. Wong, E. Joselevich, A. T. Woolley *et al.*, Nature (London) **394**, 52 (1998).